*Energy Equip. Sys. / Vol. 9/No. 2/June 2021/ 145-158*

ENERGY EQUIPSYS

**Energy Equipment and Systems**

http://energyequipsys.ut.ac.ir
www.energyequipsys.com

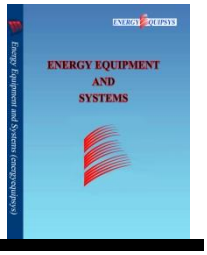


# Experimental and numerical investigation of the effects of preheating temperature on cutting force, chip shape and surface roughness in hot turning of AISI630 hardened stainless steel

**Authors**

**Mohammadjafar Hadad** [a*]
**Seyed Mohammad Ebrahimi** [a]
**Alireza Araee** [a]

[a] School of Mechanical Engineering, College of Engineering, University of Tehran, P.O. Box 11155/4563, Tehran, Iran

*Article history*:

Received : 7 March 2020
Accepted : 17 May 2020

**ABSTRACT**

*Hot machining is a type of cutting operation that an external heat source is used to pre-heat and consequently reduce the yield strength of the workpiece material. In this study, the conventional and hot turning of AISI630 hardened stainless steel, which is widely used in energy equipment, aerospace, and petrochemical industries, have been evaluated in both numerical and experimental methods. Simulation of the turning process is carried out by finite elements method (FEM) using AdvantEdge software. To predict chip morphology and cutting forces, the 2D and 3D FEM analyses have been used, respectively. The numerical analysis showed that hot turning in 300°C causes a reduction of 28% in cutting forces and consequently decreases stressed on the cutting tool. It is found that the main factor affecting the fluctuations of the cutting forces in turning of hardened AISI630 is the saw-tooth formation phenomenon (chip segmentation) as well as the shear band generation due to thermal softening of the workpiece material. Furthermore, the relation between cutting force fluctuation and the machined surface roughness has been investigated applying numerical analysis and experimental data. The results of roughness measurement revealed that hot turning in 300°C reduces the machined surface roughness up to 23%. In addition, it has been observed that hot turning technique decreases side flow and surface damages in comparison to conventional turning.*

**Keywords:** Hot Turning, Surface Roughness, Finite Elements Method, Cutting Force Fluctuation, Tool Wear.

## 1. Introduction

Machining operation is one of the manufacturing processes which is used widely in all industries in the production of various parts. In recent years, this process has received a lot of attention in terms of economy and sustainability in order to increase its efficiency. By changing the input parameters of the process, such as cutting speed, feed rate, and depth of cut, the optimized performance and sustainability can be achieved. Reduction of cutting fluid consumption, decreasing cutting tool consumption, reduction of process power consumption and increasing productivity are among the characteristics of a sustainable machining process. In other words, chip formation mechanism, as well as chip type, are

* Corresponding author: Mohammadjafar Hadad
School of Mechanical Engineering, College of Engineering, University of Tehran, P.O. Box 11155/4563, Tehran, Iran
Email: mjhadad@ut.ac.ir

other issues that should be considered in sustainable cutting processes. To this end, various methods have been developed, including optimizing the dry machining process as well as minimum quantity lubrication-MQL machining techniques. In dry machining, due to the lack of cutting fluid in the cutting area, cooling and lubrication of the process is not done well and therefore leads to tool wear and an increase of power consumption. Therefore, although dry machining is acceptable from economically and environmentally standpoints, it does not create suitable conditions in terms of process performance. Additionally, machining of some hard-to-cut materials, such as martensitic steels, superalloys, and titanium alloys, is associated with tool wear and poor surface quality**.** Therefore, to increase the efficiency of the dry machining process, it is done in combination with or the assistance of other physical/electrical/chemical/thermal processes. Today, many researchers use a new method for machining these metals called hot machining or thermally assisted machining. In this method, the workpiece is preheated by means of some equipment such as plasma arc, laser beam, gas flame, induction furnaces, and elemental furnaces [1-3]. Preheating the workpiece reduces the strength and strain hardening of the metal and therefore, reduces the cutting forces [4]. The reduction of cutting forces reduces the tool wear, but despite the force reduction in this process, with the workpiece temperature rise the tool temperature increases and consequently increases the tool wear. Some researchers performed the hot machining process experimentally on hard-cutting metals, and in most cases, tool wear and surface roughness were studied [5-7]. Others also looked at the process of hot machining utilizing numerical simulation. Germain et al. [8] simulated the conventional and hot machining of 42CrMo4 steel using FEM. Their results indicated that the shear plane angle in the hot machining is reduced, and the cutting force is reduced by a maximum of 34% compared with conventional machining. Xi et. al. [9] simulated the hot machining process of titanium alloy using the smoothed particle hydrodynamics method. They calculated the cutting force and compared it with the experimental results. In addition, they studied the formation of the saw tooth chip. A few studies have been carried out on the conventional machining of AISI630 steel. Chein and Tsai [10] provided a model for predicting flank wear and the optimum cutting conditions. Mohanty et al. [11] investigated the effects of cutting speed on tool wear and machined surface roughness. Sivaiah and Chakradhar [12] also measured the tool wear and surface roughness in dry turning and compared their results with the corresponding values for wet and MQL turning. Khani et al. [13] performed the hot turning of AISI630 steel using a plasma arc. It has been shown that hot machining at temperature 200°C increases the tool wear, but if the tool is cooled simultaneously by a cryogenic system, the tool wear decreases. Bermingham et al. [14] performed the laser-assisted milling of AISI630 steel. Their results showed that hot milling reduced the tool wear by 50% compared to conventional milling.

There is a lack of study in the field of hot turning of hardened AISI630 stainless steel. Most studies examined specific cutting tools and machining parameters, although 2D and 3D simulations of chip formation of AISI630 stainless steel have not been fully addressed. Therefore, it is necessary to investigate the effects of workpiece initial temperature and different machining parameters on the hot machining performance. In this paper, the conventional and hot turning process was carried out at 25°C, 200°C and 300°C on a precipitation AISI630 hardened stainless steel. The turning process was simulated 2D and 3D FEM using AdvantEdge software. Average cutting force and the amplitude of cutting force fluctuation have been calculated using simulation results. The relation between cutting force fluctuation and machined surface roughness has been investigated by the results of numerical analysis and experimental data.

## 2. Experimental setup

The settings of machining parameters used in the present study are summarized in Table 1. AISI630 hardened stainless steel bars with solution condition and hardness of 38HRC were prepared. After one-hour aging treatment at 482°C (900°F) in the furnace the specimens' hardness has been increased to 47±1 HRC and

**Table 1.** Machining conditions

| | |
|---|---|
| **workpiece material and dimensions** | AISI630 hardened stainless steel with 47±1 HRC (⌀35 mm x 240 mm) |
| **cutting tool inserts** | SANDVIK DNMG150608 Grade GC1115 |
| **tool holder** | PDJNR2525M1506 |
| **cutting tool geometry** | rake angle= -6°, clearance angle=6°, nose radius=0.8mm, cutting edge radius=0.02mm, major cutting edge angle=93° |
| **process parameters** | cutting speed ($V_c$)= 62, 96, 123 m/min<br>feed ($f$)= 0.102,0.175,0.241 mm/rev<br>depth of cut ($d$): 0.9 mm |
| **workpiece initial temperature** | T= 25°C, 200°C, 300°C |
| **Environment/coolant-lubricant** | dry turning (conventional turning)<br>dry hot turning (hot turning) |

their structure changed to H900 (according to ASTM A564 standard). All machining experiments have been conducted on bars 35mm in diameter and 240mm in length for 3 minutes. SANDVIK DNMG150608 Grade GC1115 cutting tools (with rake angle of -6° and clearance angle of 6° (Fig.1)) and PDJNR2525M1506 tool holder have been used for turning experiments. The main cutting edge angle of 93° and the cutting depth of 0.9mm was kept in all machining experiments (Fig.1).

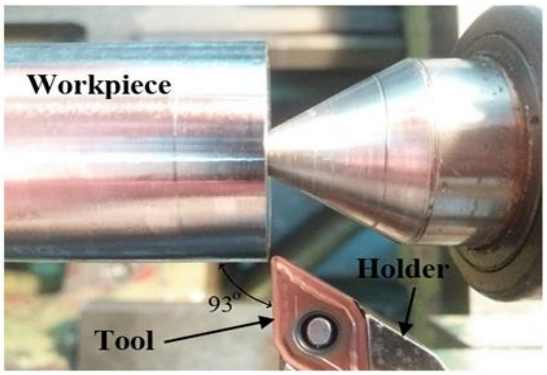


**Fig.1**: Tool and workpiece set-up

The cutting edge radius, as well as nose radius, were 0.02 mm and 0.8 mm, respectively. The feed was set at 0.102, 0.175, and 0.241 mm/rev. Turning was carried out at 25°C, 200°C and 300°C. To carry out hot turning for example at 300°C, the workpiece was first incubated in a furnace at 350°C for 45 minutes. The workpiece has been mounted on the lathe (Fig.2) after exiting the furnace for about 30 seconds.


**Fig.2**: Lathe and furnace used for hot turning

Then the turning process was performed for three minutes. The workpiece surface temperature was measured at intervals of 15 seconds using a contact thermocouple type CHY-502A (Fig. 3a) and plotted in a diagram shown in Fig. 3b. In addition, the simulation of temperature drop was performed using Fluent software, and it was observed that after three minutes, a maximum of 50°C temperature drop occurred at the workpiece surface. The reason for the low-temperature drop is the low conductivity of AISI630 stainless steel. The conductivity of AISI630 is 17 W/m°C at ambient temperature, while the conductivity of low carbon steel is 48 W/m°C**.** As shown in Fig.3b, the hot turning process was performed in the temperature range of 300-330°C because of the short machining time. Machined surface roughness was measured applying HOMMELWERKE Turbo Roughness V3.34 surface roughness tester. The microstructure of

the chip and its dimensions were investigated using OLYMPUS BH2-UMA optical microscope. To evaluate the microstructure of the chips' cross-section, fry's reagent (5gr CuCl2, 40mL concentrated HCl, 30mL methyl, 30mL $H_2O$) was used for etching. The microstructure of the machined surfaces and the cutting tool wear was investigated using a scanning electron microscope (SEM).

## 3. Finite element model of turning process

Numerical analysis was performed using FEM using AdvantEdge software [15]. A validated FEM model was used for simulation [16]. The turning process was simulated in both 2D and 3D environments. To predict the chip morphology a two-dimensional analysis of the turning process has been made. This assumption is acceptable especially in predicting the chip morphology [5, 17]. The tool was kept constant during the analysis, and the workpiece was displaced to the tool with constant cutting speed $V_c$, as shown in Fig.4. The cutting tool has been considered rigid with a cutting edge radius of 0.02 mm (Fig.4). The thermal conductivity of the tool was considered 100 W/m°C. The friction coefficient between the tool rake face and the chip was considered 0.5. Conductivity and specific heat of the hardened AISI630 steel were considered to be 17 W/m°C and 500 J/kg°C, respectively. Numerical analysis was performed as a thermo-mechanical coupling. In 2D model, the number of elements of the workpiece was 30,000 and the size of the

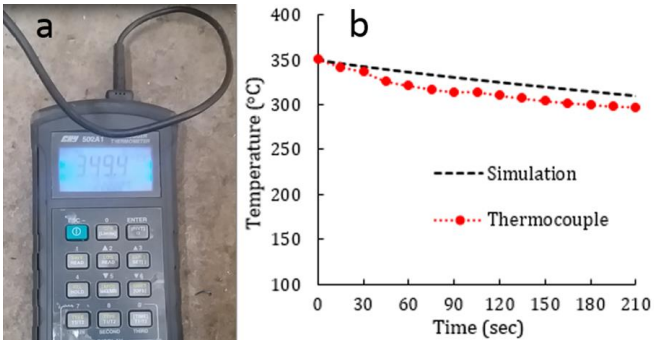


**Fig. 3**: a) contact thermocouple CHY-502A, b) workpiece surface temperature versus time

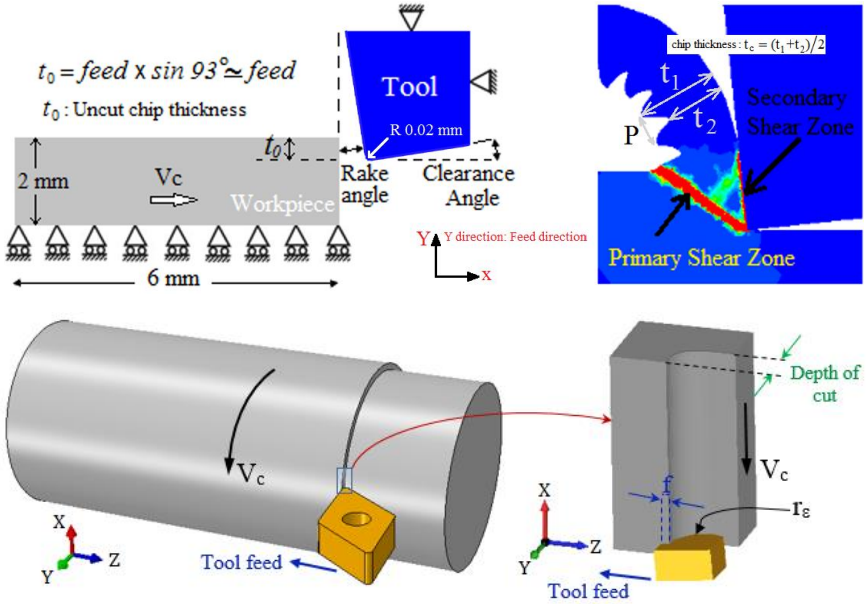


**Fig.4**: Two-dimensional (top) and three-dimensional (bottom) model of turning process in finite elements analysis

smallest and largest side of the elements in the primary and secondary shear zones were 7 microns and 80 microns, respectively. During the finite element analysis, AdvantEdge automatically uses the adaptive remeshing process in the primary and secondary shear zones. To obtain the correct results from numerical analysis of the turning process, the precise determination of the properties of the workpiece material, especially the flow stress under high strain, high strain rate and high temperatures, is required**.** In this paper, Power Viscosity Law (PVL) model [15] was used as a constitutive equation for the flow stress behavior of AISI630 hardened stainless steel. This model is expressed by Eq. (1):

$$\sigma(\varepsilon^p, \dot{\varepsilon}, T) = \sigma_0 \left(1 + \frac{\varepsilon^p}{\varepsilon_0^p}\right)^{\frac{1}{n}} \times \left(1 + \frac{\dot{\varepsilon}}{\dot{\varepsilon}_0}\right)^{\frac{1}{m}} \times (C_0 + C_1 T + C_2 T^2 + C_3 T^3) \quad (1)$$

The first term in Eq.(1) describes the strain-hardening behavior of metal. Where $\sigma$ is flow stress, $\sigma_0$ is initial yield strength, $\varepsilon^p$ is plastic strain, $\varepsilon_0^p$ is reference plastic strain and *1/n* is strain-hardening exponent. The second term describes the behavior of the metal at high strain rates. $\dot{\varepsilon}$ is the plastic strain rate, $\dot{\varepsilon}_0$ is reference plastic strain rate and $m_1$ is strain rate sensitivity coefficient. The third term represents the thermal softening behavior of metal. $C_0$ to $C_3$ are the constants of the thermal softening equation. T is the temperature of the metal at each increment. The constants parameters of PVL models are shown in Table 2 [16].

## 4. Results and Discussion

### 4.1. Effects of preheating temperature on machining forces

As the initial temperature of the workpiece increases, the average value of the cutting force decreases. Cutting forces are shown in Fig.5 for conventional and hot turning operations in a cutting speed of 96 m/min and feed of 0.175 mm/rev. It can be seen that the cutting force plot is fluctuating versus time for both conventional and hot turning processes. The main reason is the chip formation mechanism of this steel. The average cutting force in conventional turning is 530 N, however it is reduced to 384 N in hot turning operation at pre-heating temperature of 300°C. The amplitude of the cutting force fluctuations ($\Delta F_c$) as Peak-to-Peak has been shown in Fig.5.

**Table 2.** Constants of the PVL model for hardened AISI630 [16]

| $\sigma_0$ (MPa) | ***n*** | $\varepsilon_0^p$ | ***m1*** | $\dot{\varepsilon}_0$ |
|---|---|---|---|---|
| 1370 | 18 | 0.0015 | 179 | 0.001 |
| **T cut**(°C) | ***C0*** | ***C1*** | ***C2*** | ***C3*** |
| 750 | 1.01 | -5.54E-4 | -2.63E-7 | -5.23E-10 |

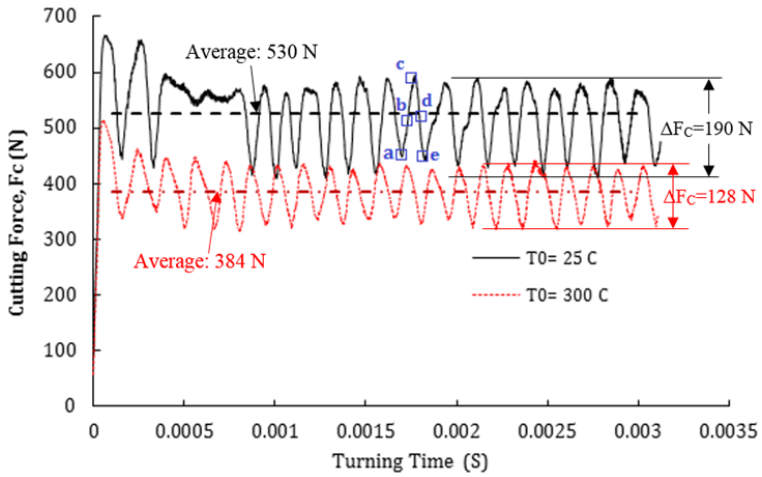


**Fig.5:** Calculated cutting force in conventional and hot turning for $V_c$=96 m/min and f= 0.175 mm/rev

It can be seen that, in addition to decreasing the average cutting force, the amplitude of the cutting force oscillations is reduced in hot machining in comparison to the conventional turning. The influence of the initial workpiece temperature on the cutting forces is shown in Fig.6. It is shown that compared to conventional turning, hot turning at 200°C and 300°C reduces the cutting forces by 19% and 28%, respectively. The amplitude of the cutting force fluctuation has been calculated using finite element analysis (Fig.7). Moreover, Fig.7 shows that with increasing initial cutting temperature and cutting speed, the amplitude of cutting force fluctuation decreases. In addition, the amplitude of fluctuation increases with increasing feed. It is observed that hot turning reduces the amplitude of cutting force fluctuation by 37%.

### 4.2. Investigation of the saw-tooth chip formation mechanism

Due to the low thermal conductivity and high strength of AISI630, the obtained chips are mainly saw-tooth type. Therefore, it is expected that the cutting force fluctuates with the machining time. In addition, a segment or tooth formation, as well as the shear stress contour, have been shown in Fig.8. In Fig.8a, segment A has been formed and the applied force on the cutting tool is at its minimum value at point "a" shown in Fig.5. As the workpiece feeds toward the cutting tool the material under segment A deforms (Fig.8b).

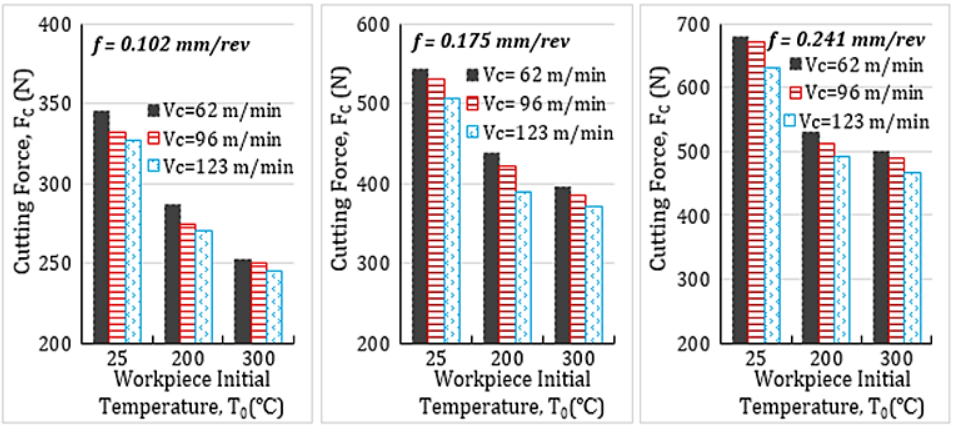


**Fig.6:** Average cutting forces calculated by 3D-FEM in conventional turning and hot turning

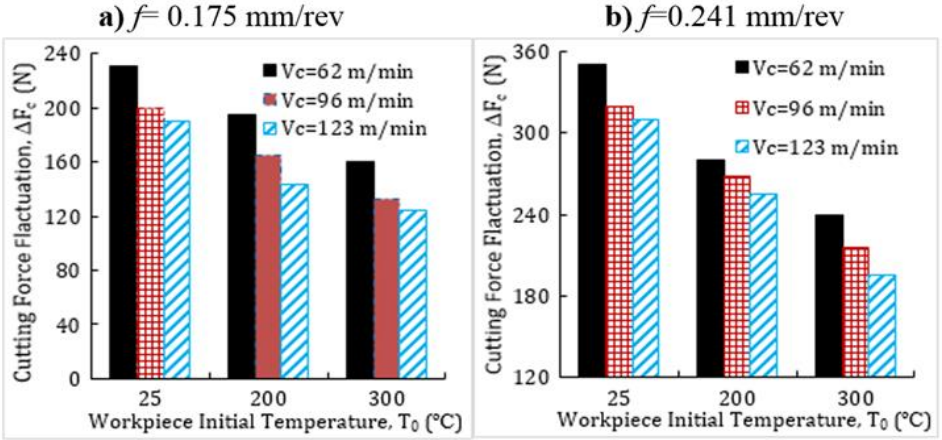


**Fig.7:** The effects of initial temperature and cutting speed on the fluctuation amplitude of the cutting force (peak to peak)

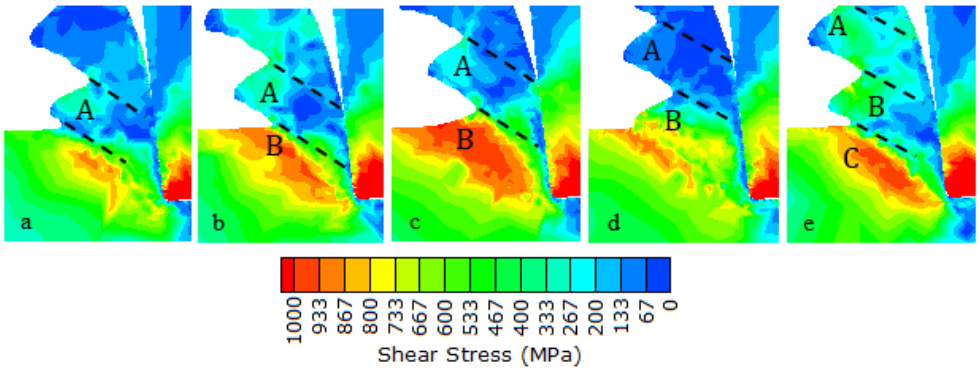


**Fig.8:** Chip formation in conventional turning at $V_c$=96 m/min and f= 0.175 mm/rev

This deformation is the base of new segment formation called B. At this step, the applied force on the cutting tool increases slowly (point "b" in Fig.5). As the workpiece moves continuously toward the tool, the bulk workpiece material on the rake face of cutting tools will undergo severe shear deformation (Fig.8c) and the applied force on the cutting tool edge reaches its maximum value (point "c" in Fig.5). By increasing deformation in the initial deformation zone, the local temperature at this area increases and consequently results in material softening. This phenomenon causes local deformation and the beginning of shear banding. Therefore, the metal is deformed with lower force at the shear zone and the force is reduced compared to the previous step (point "d" in Fig.5). As the deformation and strain of metal increase, the damage mechanism results in cutting the material (Fig.8d). By continuing the cutting process, the local deformation along the shear zone proceeds with lower force and segment B is fully formed (Fig.8e). For this case, the force diagram at point "e" is shown in Fig.5. As segment B is completed, new segment C begins to form.

In order to understand the formation of the shear band phenomenon in the turning of AISI630 hardened stainless steel, the chips obtained under conditions of Figs. 5 and 8 were mounted, followed by polishing with soft grains and alumina powder, and the cross-sectional microstructure images were observed after Fry's reagent etching. The shear bands are shown in Fig.9. Areas that undergone low plastic deformation are shown with the Low Strain phrase, where they have larger grain sizes. In other words, the grains are fine and long in the areas where the shear band phenomenon occurred. An example for these areas is represented by the phrase High Strain in Fig.9.

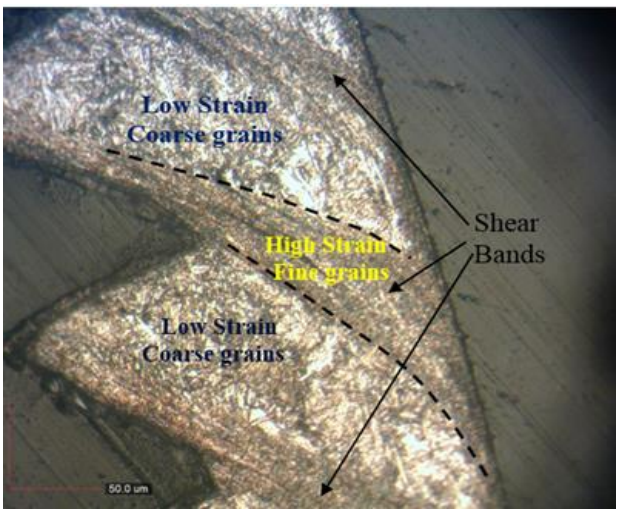


**Fig.9:** formation of shear bands in conventional turning at $V_c$=96 m/min and f= 0.175 mm/rev

Figure 10 compares the geometry and dimensions of the chips obtained from finite element analysis and experiments. However, the plastic strain contour shown in Fig.10 indicates that the local deformation on the shear plane applies higher strains in some areas and results in chip segmentation. Higher strains are in the areas marked with red and green colors, while lower strains are applied on other areas shown in blue which is consistent with the Low Strain areas defined in Fig.9.

### 4.3.Effects of preheating temperature on chip shape

The effects of the initial workpiece temperature on the chip shape are illustrated in Fig.11 using finite element analysis. By increasing chip temperature, the distance between the two successive shear planes which is the saw tooth pitch (P) increases. Figure 12 shows the obtained chips from conventional and hot turning operations.

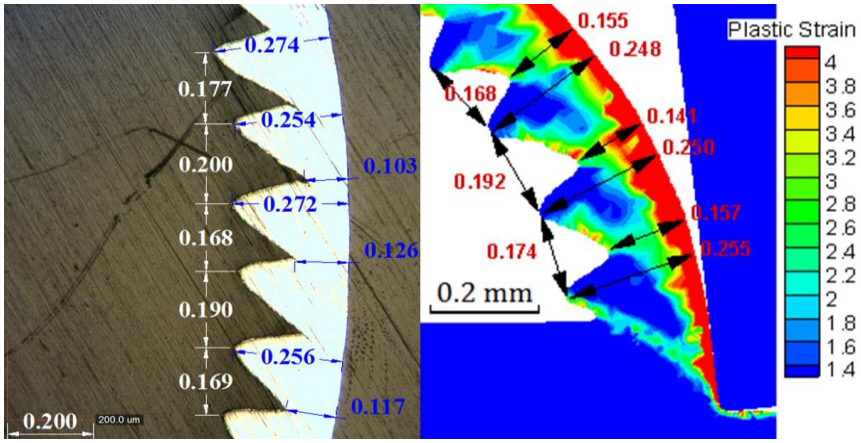


**Fig.10:** Comparison between experimental (left) and numerical results (right). Strain localization and formation of shear bands in conventional turning at $V_c$=96 m/min and f= 0.175 mm/rev.

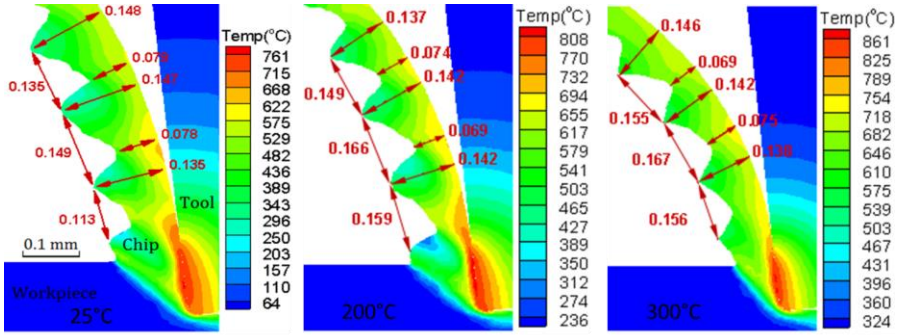


**Fig.11:** Predicted chip forms for turning under different workpiece initial temperatures and $V_c$=123 m/min and f= 0.102 mm/rev

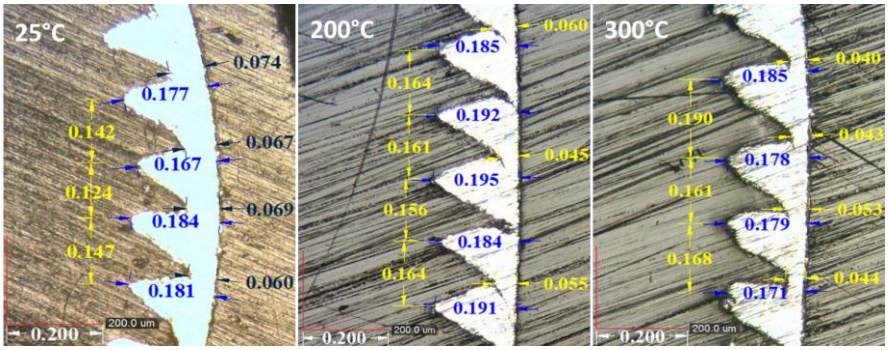


**Fig.12:** Chips obtained from conventional and hot turning operations with $V_c$=123 m/min and f= 0.102 mm/rev

### 4.4.Effects of preheating temperature on fluctuation frequency of cutting force

In addition to affecting the force fluctuation amplitude, hot turning also influences the force fluctuation frequency. The main fluctuation frequency of cutting forces can be calculated using the Fast Fourier Transform (FFT). Moreover, the chip segmentation frequency should be calculated to find the origin of these fluctuations and their relations to the shear band formation on the shear plane as well as the formation of segmented/saw tooth chip. The chip segmentation frequency can be obtained using Eq. (2) [17]:

$$f_{CS} = \frac{100 V_S}{6 P} \tag{2}$$

where $f_{CS}$ is Chip segmentation frequency or frequency of the formation of shearing planes determined from chip geometry, $V_S$ is the chip slip speed on the tool rake face and $P$ is the distance between two consecutive shearing planes measured in the direction of the tool rake face (Fig.4). $Vs$ (m/min) is given by Eq. (3) as [17]:

$$V_S = V_C \frac{f.a_p}{t_C\, l_C} \tag{3}$$

where $V_C$ is the cutting speed (m/min), $f$ is the feed rate (mm/rev), $a_p$ is the depth of cut (mm), $t_C$ is the mean chip thickness (mm) and $l_C$ is the width of the chip (mm). The cutting force fluctuation frequency ($f_{CF}$) has been calculated using Fast Fourier Transform (FFT) in FE simulation. For example, Fig.13 shows the FFT of cutting forces calculated in Fig.5. It can be seen that there is a peak at a frequency of 6402 Hz, which is the same as the main frequency of cutting force fluctuation. The chip segmentation frequency extracted from the experimental and simulated chip forms is compared with the simulated cutting force frequency. It is indicated that the values of chip segmentation frequency are close to the cutting force fluctuation frequency, and both frequencies reduction in a similar way with increasing workpiece initial temperature. Therefore, it can be concluded that the main factor affecting the cutting force fluctuations in Fig.5 is the saw-tooth formation as well as the shear band generation due to thermal softening. As shown in Fig.14, the frequency of cutting force fluctuation decreases with increasing workpiece initial temperature.

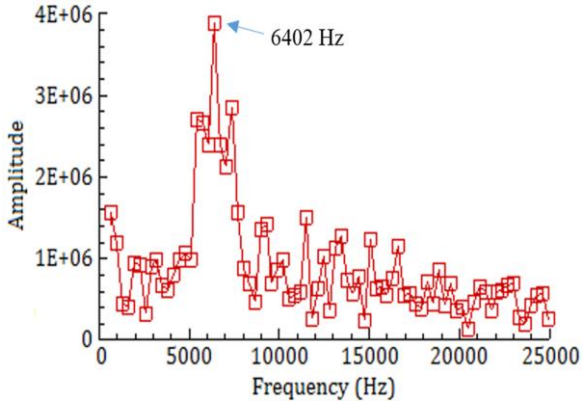


**Fig.13:** FFT representation of cutting force in conventional turning for $V_c$=96 m/min and f=0.175 mm/rev

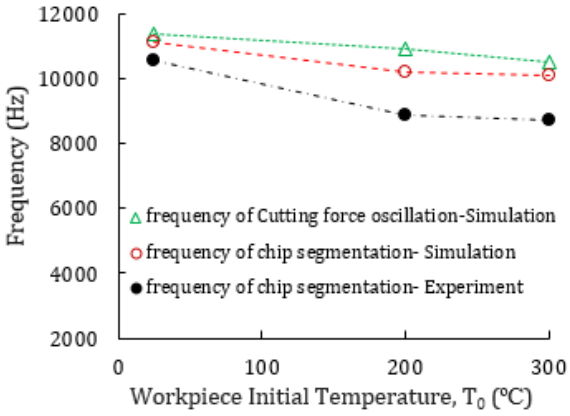


**Fig.14:** Comparison of the frequencies of the force oscillation and the chip segmentation in conventional and hot turning for $V_c$=123 m/min and f=0.102 mm/rev

### 4.5.Effects of preheating temperature on surface roughness

The roughness profiles are shown in Figure 15 in conventional and hot turning at 300 ºC for a cutting speed of 62 m/min and a feed of 0.241 mm/rev. The effects of initial temperature and cutting parameters on the workpiece surface roughness are shown in Fig.16. It can be seen from this figure that the machined surface roughness decreased during hot turning at 300 ºC up to 23%, 20% and 11% compared to conventional turning at feeds of 0.102, 0.175, and 0.241 mm/rev, respectively. By increasing the workpiece initial temperature in hot turning, the temperature rise in the primary shear zone will be increased. Therefore, the hardness and strength of the uncut chip will be reduced and as a result cutting forces will be decreased. Therefore, workpiece surface roughness is reduced and the efficiency of the cutting process will be increased. Another reason for surface roughness reduction in hot turning is the reduction of cutting force oscillation ($\Delta F_c$) during hot machining compare to conventional turning operation (Figs. 5 and 7). Calamaz et al. [18] observed that when saw-tooth chips are formed, the cutting tool is under cyclic deflection with a frequency close to the fluctuation frequency of the cutting force. Therefore, rake angle and cutting speed will be changed locally, and accordingly, the tool's cyclic deflection increases workpiece surface roughness. In hot turning not only the average cutting forces is reduced (Fig.6) but also the fluctuation amplitude of the cutting forces decreased compare to conventional turning operation (Figs. 5 and 7). Therefore, surface roughness is reduced in hot turning operation in comparison to conventional turning.

According to Fig.17 the obvious differences in the morphology of machined surfaces with different initial temperatures suggest a considerable influence of the preheating techniques on the chip-formation mechanisms. It can be observed that there are hardly any side flows and defects on surfaces machined with applying hot turning technique. However, surfaces generated under conventional turning are characterized by side flow and more surface damages. Moreover, with increasing cutting speed for each feed rate, workpiece surface roughness is reduced (Fig.15). In addition, by increasing the workpiece initial temperature in hot turning, the workpiece surface roughness decreases in comparison to conventional turning. Increasing cutting speed as well as workpiece initial temperature, the hardness and strength of the uncut chip will be reduced and as a result cutting forces will be decreased (Fig 6). Therefore, workpiece surface roughness is reduced and the efficiency of the cutting process will be increased.

### 4.6.Effects of preheating temperature on cutting tool stresses

The Von-Mises stress distribution on the cutting tool edge is shown Fig.18 for conventional and hot turning operations. As shown in Fig.18, a smaller area of the cutting tool edge is exposed to stresses more than 2800 MPa for hot turning

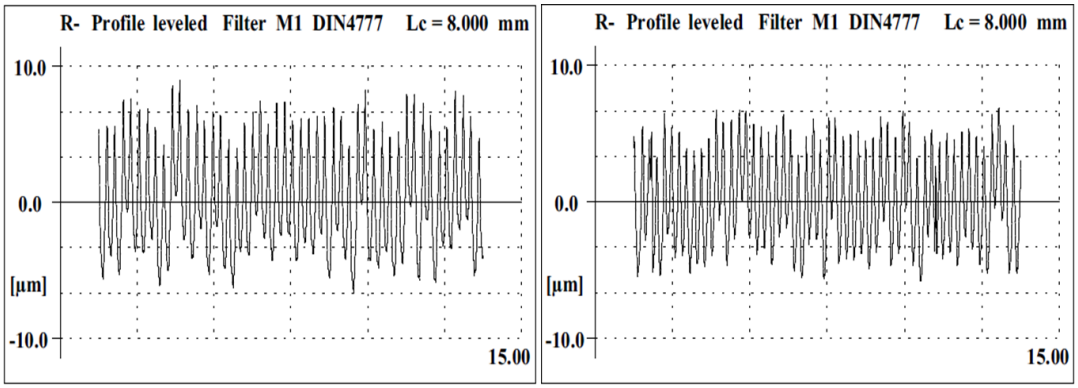


**Fig.15**: Surface roughness profile after (left) conventional and (right) hot turning at 300 ºC for $V_c$=62 m/min and f= 0.241 mm/rev

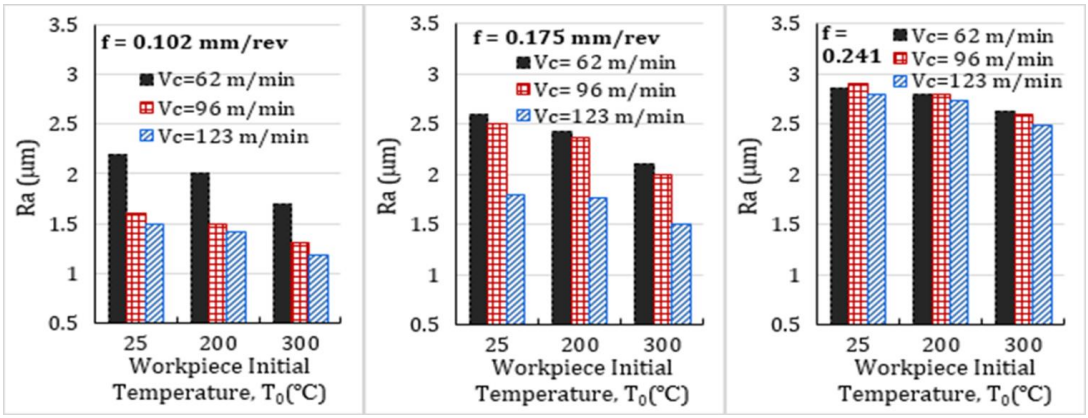


**Fig.16**: The effects of initial temperature of the workpiece and cutting parameters on the surface roughness

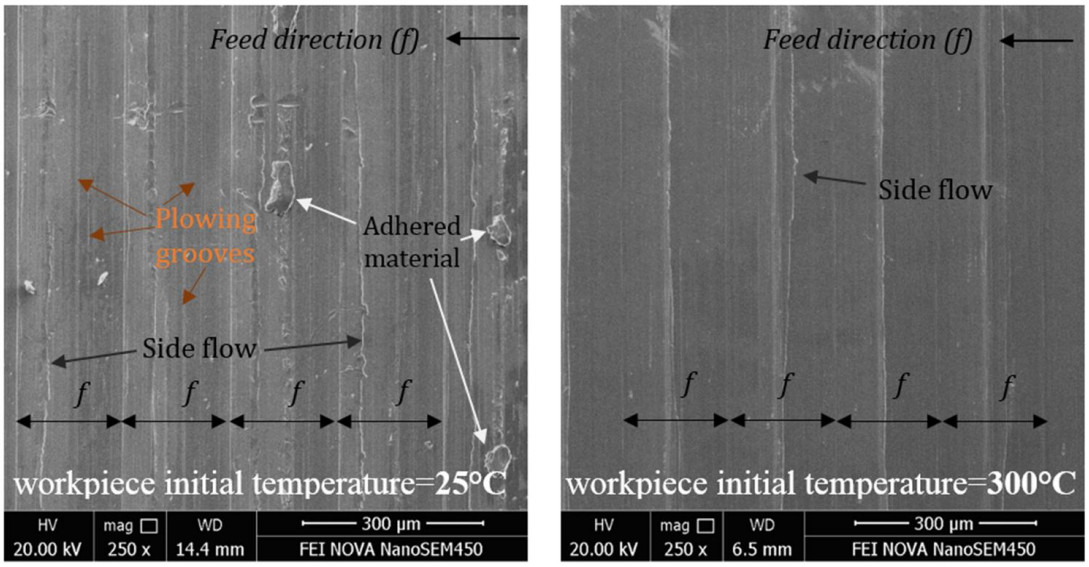


**Fig.17**: SEM micrographs of machined specimens under $V_c$=62 m/min and f=0.175 mm/rev

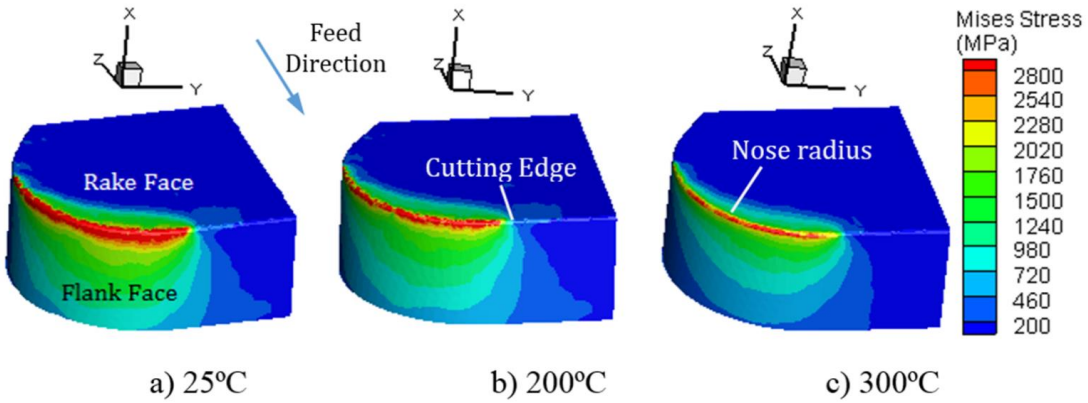


**Fig.18**: Tool stress distribution under $V_c$=62 m/min and f=0.102 mm/rev

process. In addition, for other feeds and cutting speeds, the simulation results also prove that the tool stresses in conventional turning are always higher than hot turning at 200°C and 300°C.

### 4.7. Effects of preheating temperature on flank wear

Cutting tool wear values have been measured using SEM and optical microscope after three minutes turning at ambient temperature, 200°C and 300°C. As can be found from Fig.19 that tool wear in hot turning decreased by 23% compared to conventional turning. In addition, tool wear is so severe in conventional turning that the tool coating layers are removed and the WC exposed, whereas in hot turning only the tool top coating layer was abraded. One of the reasons for the reduction of tool wear in hot turning is a 27% reduction of cutting force in comparison to conventional turning (Fig.6), which reduces the stress applied to the cutting edge (Fig.18). According to Figs. 6 and 20, the force applied to the tool during hot turning is 19% lower than that in conventional turning and therefore tool wear is reduced from 0.116mm in conventional turning to 0.099mm in hot turning. Moreover, tool wear measurement of all cutting tools shows that hot turning of AISI630 hardened steel at 200°C and 300°C reduces flank wear by 15% and 33%, respectively.

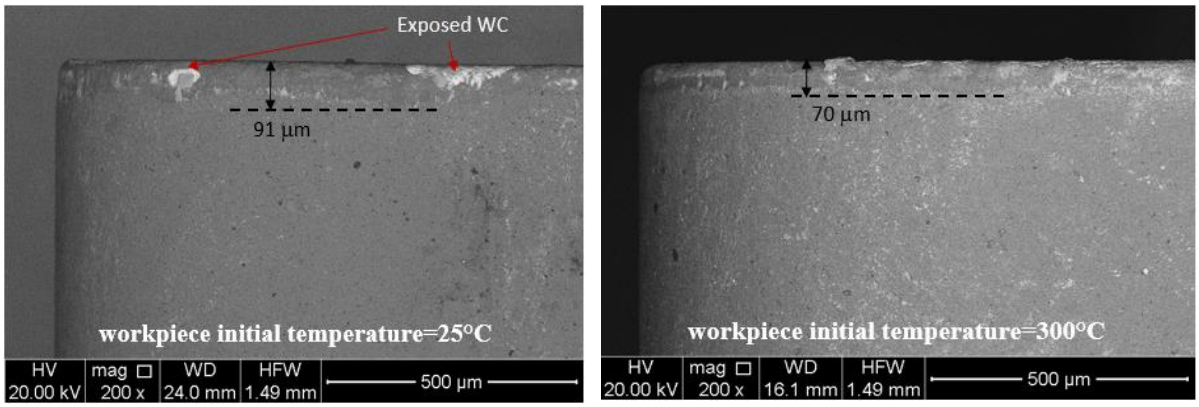


**Fig.19:** Comparison of flank wear in conventional turning and hot turning at 300ºC for $V_c$=62 m/min and f=0.102 mm/rev

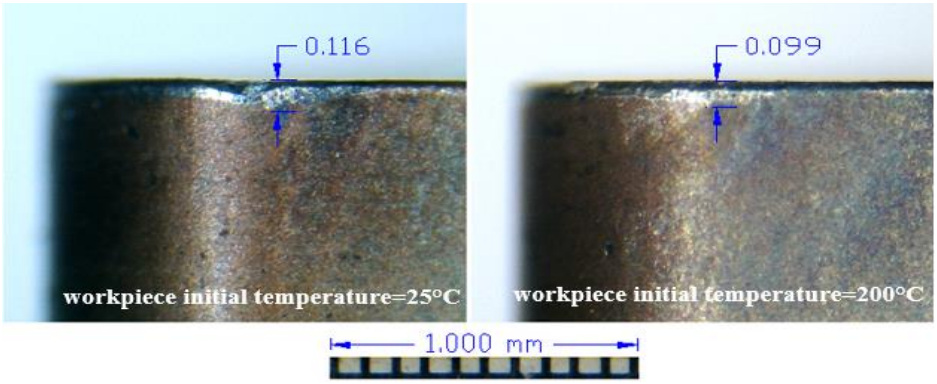


**Fig.20**: Comparison of flank wear in conventional turning and hot turning at 200ºC for $V_c$=62 m/min and f=0.175 mm/rev

## 5. Conclusion

In this research, the conventional turning and hot turning process at 200ºC and 300ºC were investigated experimentally and numerically on hardened AISI630 stainless steel. The main results of this research are:
Hot turning at 200ºC and 300ºC reduces the cutting force up to 19% and 28%, respectively and consequently, reduces the stress. Moreover, in hot turning, the

1. Fluctuation amplitude of the cutting forces decreased in comparison to conventional turning.
2. FFT analysis of cutting force shows that the main factor affecting the cutting force fluctuations is the saw-tooth chips formation as well as the shear band generation due to thermal softening of AISI630. However, by increasing the workpiece initial temperature, the saw-tooth pitch increases and the frequency of cutting force oscillation decreases.
3. Machined surface roughness decreased during hot turning at 200ºC and 300ºC up to 9% and 23% compared to conventional turning. In hot turning not only the average cutting force is reduced, but also the fluctuation amplitude of the cutting forces decreased compare to conventional turning operation. Therefore, surface roughness is reduced in hot turning operation in comparison to conventional turning.
4. Hot turning decreases the side flows and other defects on the machined surface in comparison to conventional turning. In addition, hot turning at 200ºC and 300ºC reduces the tool wear up to 15% and 33% compared to conventional turning.

## References

[1] Azhdari S, Shoja Razavi R, Vafaei R (2017) Pulsed laser-assisted machining of Inconel 718 superalloy. Optics & Laser Technology 87:72–78. https://doi.org/10.1016/j.optlastec.2016.07.020

[2] Lajis MA, Nurul Amin A, Karim ANM, Radzi H, Ginta TL (2009) Hot Machining of Hardened Steels with Coated Carbide Inserts. American J. of Engineering and Applied Sciences 2:421-442. https://doi.org/10.3844/ajeassp.2009.421.427

[3] Ha, J.H. ; Lee, C.M. (2019) A Study on the Thermal Effect by Multi Heat Sources and Machining Characteristics of Laser and Induction Assisted Milling. Materials (Basel). 12, 1032-1053. https://doi.org/10.3390/ma12071032.

[4] Ganta V, Chakradhar D (2014) Multi objective optimization of hot machining of 15-5PH stainless steel using grey relation analysis. Procedia Materials Science 5:1810-1818. https://doi.org/10.1016/j.mspro.2014.07.468

[5] Muhammad R, Maurotto A, Roy A, Silberschmidt V (2012) Hot ultrasonically assisted turning of β-Ti alloy, 5th CIRP Conference on High Performance Cutting 2012 ,Procedia CIRP 1:336-341. https://doi.org/10.1016/j.procir.2012.04.060

[6] Ginta TL, Nurul Amin A (2012) Cutting Force and Tool Life Models in End Milling Titanium Alloy Ti-4Al-4V with Thermally-Assisted Machining. Int. J. of Mechanical Computational and Manufacturing Research 1(1):1-5.

[7] Bermingham MJ, Palanisamy S, Dargusch MS (2012) Understanding the tool wear mechanism during thermally assisted machining Ti-6Al-4V. International Journal of Machine Tools & Manufacture 62(1):76-87.https://doi.org/10.1016/j.ijmachtools.2012.07.001

[8] Germain G, DalSanto P, Lebrun JL (2011) Comprehension of chip formation in laser assisted machining. International Journal of Machine Tools & Manufacture 51:230–238. https://doi.org/10.1016/j.ijmachtools.2010.11.006

[9] Xi Y, Bermingham M, Wang G, Dargusch M (2014) SPH/FE modeling of cutting force and chip formation during thermally assisted machining of Ti6Al4V alloy. Computational Materials Science 84:188–197. https://doi.org/10.1016/j.commatsci.2013.12.018

[10]Chien WT, Tsai CS (2003) The investigation on the prediction of tool wear and the determination of optimum cutting conditions in machining 17-4PH stainless steel. Journal of Materials Processing Technology 140:340–345. https://doi.org/10.1016/S0924-0136(03)00753-2

[11]Mohanty A, Gangopadhyay S, Thakur A (2015) On Applicability of Multilayer Coated Tool in Dry Machining of Aerospace Grade Stainless Steel. Materials and Manufacturing Processes 31(7):869-879. https://doi.org/10.1080/10426914.2015.1070413

[12]Sivaiah P, Chakradhar D (2017) Experimental investigation on feasibility of cryogenic, MQL, wet and dry machining environments in turning of 17-4 PH stainless steel. Materials and Manufacturing Processes 32(15): 1775-1788. https://doi.org/10.1080/10426914.2017.1339317

[13]Khani S, Farahnakian M, Razfar MR (2015) Experimental study on Hybrid Cryogenic and Plasma-Enhaced Turning of 17-4PH Stainless Steel. Materials and Manufacturing Processes 30:868–874. https://doi.org/10.1080/10426914.2014.984200

[14]Bermingham MJ, Kent D, Dargusch MS (2015) A new understanding of the wear processes during laser assisted milling 17-4 precipitation hardened stainless steel. Wear 328-329:518–530. https://doi.org/10.1016/j.wear.2015.03.025

[15]AdvantEdge 7.1 User's manual, Third Wave Systems Inc.

[16]Ebrahimi SM, Araee AR, Hadad MJ (2019) Investigation of the effects of constitutive law on numerical analysis of turning processes to predict the chip morphology, tool temperature and cutting force. Int. J. Adv. Manuf. Technol. 105: 4245–4264. https://doi.org/10.1007/s00170-019-04502-7

[17]Belhadi S, Mabrouki T, Rigal JF, Boulanouar L (2005) Experimental and numerical study of chip formation during straight turning of hardened AISI 4340 steel. Proc. IMechE Part B: J. Engineering Manufacture 219 (7):515-524. https://doi.org/10.1243/095440505X32445

[18]Calamaz M, Coupard D, Girot F (2008) A New Material Model for 2D Numerical Simulation of Serrated Chip Formation When Machining Titanium Alloy Ti–6Al–4V. International Journal of Machine Tools and Manufacture 48: 275–288. https://doi.org/10.1016/j.ijmachtools.2007.10.014